Available online at www.sciencedirect.com
ScienceDirect
Trans. Nonferrous Met. Soc. China 24(2014) 3955−3963
Transactions of Nonferrous Metals Society of China
www.tnmsc.cn

Adsorption and activation of copper ions on chalcopyrite surfaces: A new viewpoint of self-activation

Jiu-shuai DENG, Shu-ming WEN, Jian LIU, Dan-dan WU, Qi-cheng FENG

State Key Laboratory of Complex Nonferrous Metal Resources Clean Utilization,
Faculty of Land Resource Engineering, Kunming University of Science and Technology, Kunming 650093, China

Received 10 February 2014; accepted 22 October 2014

Abstract: The adsorption behaviors of copper ions on chalcopyrite surfaces were investigated based on zeta potential measurements, X-ray photoelectron spectroscopy, copper ion adsorption experiments, first-principles calculations, and Hallimond tube cell flotation experiments. The results show that copper ions activate the chalcopyrite as a result of the interactions between copper ions and sulfur on the chalcopyrite surface. This adsorption increases the flotation rate under certain conditions, and this is beneficial for the flotation of chalcopyrite. The copper ions in the flotation pulp are mainly derived from surface oxidation dissolution and the release of fluid inclusions, and these effects enable chalcopyrite to be activated.
Key words: chalcopyrite; copper ions; adsorption; self-activation

1 Introduction

Copper is a thiophilic element. Copper ion is a well-known flotation activator, especially for sphalerite and pyrite, and this property has been widely used in industry [1,2]. Many studies have focused on the mechanisms of copper ion activation of metal sulfide minerals such as sphalerite and pyrite, and nonmetallic minerals such as chlorite and quartz [2–6]. The activation of sphalerite by copper ions occurs through ion exchange, in which the Zn of sphalerite is substituted by Cu(II) at a ratio of 1:1, thereby releasing Zn^{2+} into the solution [2,4,7]. This chemical reaction can be represented by

$$ZnS_{(s)}+Cu_{(aq)}^{2+}\rightarrow CuS_{(s)}+Zn_{(aq)}^{2+} \quad (1)$$

The amount of Cu(II) on the sphalerite surface decreases gradually and is converted to Cu(I) by oxidation of surface sulfur. Collecting agent molecules such as xanthate react with the cuprous sulfide formed on the surface of the mineral, thereby promoting the flotation response [8]. Pyrite, which has inherent floatability, can also be activated by copper ions. The mechanism of activation of pyrite by copper ions differs from that of sphalerite: copper ions are adsorbed on sulfur sites on the pyrite surface [9,10]. Activation by copper ions applies not only to metal sulfide minerals, but also to chlorites, lizardite, and quartz. In the pH range of 7–10, minerals activated by copper ions interact with xanthate to achieve floatability. In this pH range, the zeta potential is affected by the addition of copper ions and hydroxyl compounds. Compared with nickel ions, copper ions are better activators of nonmetallic minerals [6].

Copper ions have an unusual activation effect, which promotes the recovery of sphalerite, pyrite, and other minerals. However, the activation effect of copper ions makes mineral separation difficult. A comprehensive study of the special characteristics, applications, and control of activation by copper ions is therefore necessary.

Copper ions are unavoidable ions in the flotation pulps of polymetallic sulfide ores. The main sources of these ions include the surface oxidation dissolution of minerals and copper ions in water [11–19]. In addition to these sources, fluid inclusions are very important sources

Foundation item: Projects (51464029, 51168020, 51404119,) supported by the National Natural Science Foundation of China; Project (2014Y084) supported by the Natural Science Foundation of Yunnan Province Education Department, China; Projects (41118011, 201421066) supported by the Cultivation Program of Kunming University of Science and Technology, China
Corresponding author: Shu-ming WEN; Tel: +86-871-65153445, E-mail: shmwen@126.com
DOI: 10.1016/S1003-6326(14)63556-1

of copper ions [20]. Previous researchers did not take account of fluid inclusions, which may introduce new components into the flotation pulp. These ions increase the complexity of the flotation pulp.

The influence of copper ions on the potential, surface properties, and flotation of chalcopyrite was investigated. Self-activation of chalcopyrite was proposed based on the experimental results, and a new explanation of chalcopyrite floatability was presented.

2 Experimental

2.1 Materials

The experimental materials were obtained from the Dongchuan copper deposits located in the midlands of Yunnan province, China. High-purity chalcopyrite crystals were obtained from the material after the manual removal of gangue minerals such as calcite and quartz. X-ray diffraction (XRD, Japan Rigaku Corporation) was performed using Cu K_α radiation (λ=1.5406 Å) at an operating voltage of 40 kV and a current of 40 mA. The diffraction angle (2θ) was scanned from 10° to 90°. The XRD pattern and chemical composition of the material are shown in Fig. 1 and Table 1, respectively.

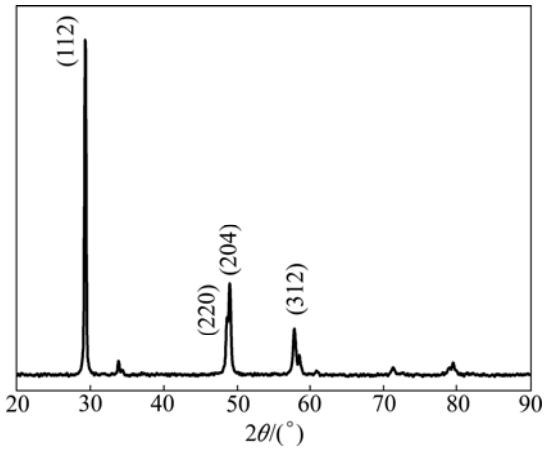

Fig. 1 XRD pattern of chalcopyrite crystal

Table 1 Chemical composition of materials (mass fraction, %)

Cu	Fe	S	SiO_2	CaO
33.24	27.22	34.81	3.23	1.50

As shown in Fig. 1, four strong peaks are observed in the XRD pattern of chalcopyrite, consistent with those the powder diffraction standards card (No. 37−0471). The values of the lattice constants are as follows: a=b=5.2864 Å, c=10.4102 Å, α=β=γ= 90°, confirming that chalcopyrite has a tetragonal structure. Although impurities are present in the chalcopyrite, as shown in Table 1, they are not detected in XRD pattern because of their very low contents. The combined results in Fig. 1 and Table 1 show that the chalcopyrite has high purity.

The deionized water used in the experiment was obtained using a Milli-Q5O system. The reagents used in the experiments were AR-grade hydrochloric acid, sodium hydroxide, and copper sulfate.

2.2 Zeta potential analysis

The chalcopyrite (particle size approximately 1 mm) was cleaned with deionized water, and then air-dried in a glove box under argon gas. Dried pure mineral (14 g) was weighed for each experiment, placed in two ball-milling jars of the same model, and then installed in closed ball-milling pots on an impacted ball-milling instrument (MM400, Retsch, Germany). The vibration frequency was set at 900 min^{-1} and the grinding time was set at 8 min.

Zeta potentials were measured using a ZetaProbe instrument (Colloidal Dynamics Company, USA), which used multiple-frequency electric acoustics. To ensure the accuracy of the measurements, a standard solution was used to calibrate the conductivity, potential, pH value, and temperature. The density, dielectric constant, and mass fraction of the sample, and the density, viscosity, and dielectric constant of water were input into the instrument's TabControl operator. In each experiment, the ground sample was quickly placed into a measuring cup filled with deionized water, and the content of the sample solution was made up to 5%. The stirring speed was set at 200 r/min. Hydrochloric acid solution (2 mol/L) and sodium hydroxide solution (2 mol/L) were used as titrants.

After calibration, the potential, conductivity, and pH of the standard solution were consistent with the standard values. The isoelectric point (IEP) of chalcopyrite corresponded to a pH of about 2.4, consistent with the IEP values reported in the literature, which ranged between pH 2 and 3 [21,22]. This result indicated that the instrument had high precision, and chalcopyrite was an ideal experimental material.

2.3 Determination of copper ions adsorbed on chalcopyrite surface

$CuSO_4·5H_2O$ was added to the aqueous solution to yield a final Cu^{2+} concentration of 1.10×10^{-4} mol/L. Fresh ball-milled chalcopyrite (1 g) was added to 20 mL of Cu^{2+} solution. Adsorption experiments were carried out in sealed vials for different lengths of time. A centrifuge (TL−4.7W, SCI, China) was used for solid–liquid separation, and the residual copper ion content of the supernatant was measured using inductively coupled plasma atomic emission spectroscopy. Solid samples were analyzed using X-ray photoelectron spectroscopy (XPS).

2.4 XPS analysis of copper ions adsorbed on chalcopyrite surface

A solid sample with a copper ion adsorption time of 30 min was subjected to XPS analysis (Kratos Amicus, UK). An anode Mg K_α source was used, at an operating voltage of 12 kV and a power of 180 W.

2.5 Computational details

The Vienna ab initio simulation package was used for the calculations [23–25]. The chalcopyrite (001) surface was used for surface structure calculation. All calculations were performed within the generalized gradient approximation proposed by PERDEW et al [26,27]. The projector augmented wave was used to describe electron–ion interactions [25,28]. The plane wave expansion was adopted for the Kohn–Sham wave function of the valence electron [25,28,29]. The Monkhorst–Pack method was used for the *K*-point grids in the Brillouin zone [29]. A linear tetrahedron with Blöchl correction was used to calculate the total system energy [30]. The Hellman–Feynman force field was used to optimize the ground-state atomic configurations [31]. The cutoff energy for the chalcopyrite structure was 500 eV. The *K*-point grids were 7×7×3. For the (001) surface structure, a 2×2 supercell was selected for directions *a* and *b*, with eight atom layers in direction *c*. The vacuum thickness was 15 Å. An adsorbate molecule was introduced into the optimized structure during the calculation. The *K*-point grids were 3×3×1 in the Brillouin zone. The cutoff energy was 500 eV. Convergence tests were conducted by changing the sampling point density and the cutoff energy of the *K*-space.

2.6 Effect of copper ion adsorption on chalcopyrite flotation

Experiments were performed on two groups. One group consisted of freshly ground untreated samples, and the other group consisted of samples that had interacted with copper ions. A Hallimond tube cell was used to investigate the copper activation of chalcopyrite.

For one group, mineral (1 g), deionized water (20 mL), and ethyl xanthate (1 mL, 1.5×10^{-4} mol/L) were added to a 25 mL beaker. The solution was stirred with a mechanical agitator at a speed of 1000 r/min for 3 min. The solution was then transferred to a single-bubble tube. For the other group, mineral (1 g) and Cu^{2+} solution (20 mL, 1.10×10^{-4} mol/L) were added to a 25 mL beaker. The solution was stirred with a mechanical agitator at a speed of 1000 r/min for 5 min or 20 min. The solution was then transferred to a single-bubble tube. After flotation, the concentrate and tail products were filtered, dried, and weighed.

3 Results and discussion

3.1 Zeta potential analysis

The zeta potential reflects the surface charge state of charged particles and is affected by the surface properties, solution concentration, pH, temperature, and other factors [32]. In aqueous solution, zeta potentials change with ion type and concentration, and then stabilize. Ions influence the zeta potential, and therefore change the surface charges of sulfide minerals [21,33]. Previous studies have mainly focused on IEP, particularly on the impact of different experimental conditions on the IEP. HEYES and TRAHAR [34] studied potentials in relation to time in a chalcopyrite flotation pulp under different conditions. They investigated the influences of quartz and the atmosphere (air and nitrogen) on flotation and Pt electrode potentials. At pH 12, KCN, which inhibited chalcopyrite flotation, decreased the Pt electrode potential.

Studies have shown that an aqueous solution of Cu^{2+} formed four types of copper hydroxyl complex, i.e., $Cu(OH)^+$, $Cu(OH)_2$, $Cu(OH)_3^-$, and $Cu(OH)_4^{2-}$, and they undergo associated ligand reactions. The step-by-step accumulation constants of these reactions are expressed as follows [35]:

$$Cu^{2+}+OH^- = Cu(OH)^+,\ \beta_1=\frac{c_{Cu(OH)^+}}{c_{Cu^{2+}}c_{OH^-}}=10^{6.3} \quad (2)$$

$$Cu^{2+}+2OH^- = Cu(OH)_2,\ \beta_2=\frac{c_{Cu(OH)_2}}{c_{Cu^{2+}}c_{OH^-}^2}=10^{12.8} \quad (3)$$

$$Cu^{2+}+3OH^- = Cu(OH)_3^-,\ \beta_3=\frac{c_{Cu(OH)_3^-}}{c_{Cu^{2+}}c_{OH^-}^3}=10^{14.5} \quad (4)$$

$$Cu^{2+}+4OH^- = Cu(OH)_4^{2-},\ \beta_4=\frac{c_{Cu(OH)_4^{2-}}}{c_{Cu^{2+}}c_{OH^-}^4}=10^{16.4} \quad (5)$$

where β_1, β_2, β_3, and β_4 are the cumulative stability constants for Eqs. (2)–(5), and c represents the concentration of the respective components. Based on mass conservation, the total concentration of copper in the solution can be expressed as

$$c_{Cu_T}=c_{Cu^{2+}}+c_{Cu(OH)^+}+c_{Cu(OH)_2}+c_{Cu(OH)_3^-}+c_{Cu(OH)_4^{2-}} \quad (6)$$

where c_{Cu_T} is the total concentration of copper in all forms in the aqueous solution. Substitution of Eqs. (2)–(5) in Eq. (6) gives

$$c_{Cu_T}=c_{Cu^{2+}}(1+\beta_1c_{OH^-}+\beta_2c_{OH^-}^2+\beta_3c_{OH^-}^3+\beta_4c_{OH^-}^4) \quad (7)$$

The relationship between the concentrations of hydroxide and hydrogen ions in the solution can be expressed as

$$c_{OH^-}=\frac{10^{-14}}{c_{H^+}} \tag{8}$$

Substitution of Eq. (8) in Eq. (7) gives

$$c_{Cu_T}=c_{Cu^{2+}}(1+\frac{\beta_1 10^{-14}}{c_{H^+}}+\frac{\beta_2 10^{-28}}{c_{H^+}^2}+\frac{\beta_3 10^{-42}}{c_{H^+}^3}+\frac{\beta_4 10^{-56}}{c_{H^+}^4}) \tag{9}$$

The side-reaction coefficients α_0, α_1, α_2, α_3, and α_4 represent the percentages of Cu^{2+}, $Cu(OH)^+$, $Cu(OH)_2$, $Cu(OH)_3^-$, and $Cu(OH)_4^{2-}$, respectively, in c_{Cu_T}; the percentage of each component in the aqueous solution can therefore be expressed as

$$\alpha_0=\frac{c_{Cu^{2+}}}{c_{Cu_T}}=(1+\frac{\beta_1 10^{-14}}{c_{H^+}}+\frac{\beta_2 10^{-28}}{c_{H^+}^2}+\frac{\beta_3 10^{-42}}{c_{H^+}^3}+\frac{\beta_4 10^{-56}}{c_{H^+}^4})^{-1} \tag{10}$$

$$\alpha_1=\frac{c_{Cu(OH)^+}}{c_{Cu_T}}=\frac{c_{Cu^{2+}}}{c_{Cu_T}}\times\frac{c_{Cu(OH)^+}}{c_{Cu^{2+}}}=\alpha_0\frac{\beta_1 10^{-14}}{c_{H^+}} \tag{11}$$

$$\alpha_2=\frac{c_{Cu(OH)_2}}{c_{Cu_T}}=\frac{c_{Cu^{2+}}}{c_{Cu_T}}\times\frac{c_{Cu(OH)_2}}{c_{Cu^{2+}}}=\alpha_0\frac{\beta_2 10^{-28}}{c_{H^+}^2} \tag{12}$$

$$\alpha_3=\frac{c_{Cu(OH)_3^-}}{c_{Cu_T}}=\frac{c_{Cu^{2+}}}{c_{Cu_T}}\times\frac{c_{Cu(OH)_3^-}}{c_{Cu^{2+}}}=\alpha_0\frac{\beta_3 10^{-42}}{c_{H^+}^3} \tag{13}$$

$$\alpha_4=\frac{c_{Cu(OH)_4^{2-}}}{c_{Cu_T}}=\frac{c_{Cu^{2+}}}{c_{Cu_T}}\times\frac{c_{Cu(OH)_4^{2-}}}{c_{Cu^{2+}}}=\alpha_0\frac{\beta_4 10^{-56}}{c_{H^+}^4} \tag{14}$$

Based on the relationships among Eqs. (10)–(14), we conclude that

$$\alpha_0+\alpha_1+\alpha_2+\alpha_3+\alpha_4=1 \tag{15}$$

The above equations show that the forms of Cu^{2+} presented in aqueous solution are closely related to the pH value of the solution. α_0 is then substituted into Eqs. (11)–(14). The percentages of $Cu(OH)^+$, $Cu(OH)_2$, $Cu(OH)_3^-$, and $Cu(OH)_4^{2-}$ in the solution can therefore be obtained.

Figure 2 shows a plot of α_M (M=0–4) against pH. The distribution of copper species in solution at different pH values can be obtained. Figure 2 also shows that the forms of Cu^{2+} presented in solutions with different pH values are different. At pH≤7.5, the copper in the solution mainly exists as dissociated Cu^{2+} and a small amount of $Cu(OH)^+$ and $Cu(OH)_2$, with $Cu(OH)^+$ and $Cu(OH)_2$ appearing at pH>5.5 and pH >6.5, respectively. At pH≤ 5.5, the copper in the solution exists as dissociated Cu^{2+}, and at 7.5<pH≤12.25, the copper in the solution is mainly presented as $Cu(OH)_2$ and a small amount of $Cu(OH)_2$, Cu^{2+}, $Cu(OH)^+$, $Cu(OH)_3^-$, and $Cu(OH)_4^{2-}$. When the solution pH is in the range of 9<pH<11, the $Cu(OH)_2$ content is more than 95%. At pH>12.25, copper is presented mainly in the form of $Cu(OH)_4^{2-}$, with a small amount of $Cu(OH)_3^-$ and $Cu(OH)_2$. The percentage of $Cu(OH)_4^{2-}$ reaches 87% at pH=13.

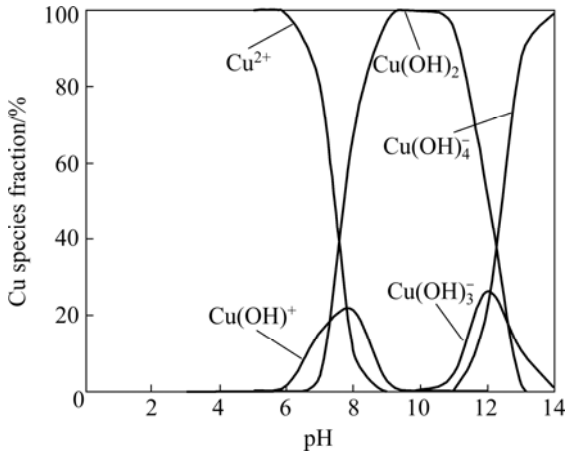

Fig. 2 Copper species fraction versus solution pH

These results are similar to those published previously [36]. Figure 2 can be used to determine the concentrations of copper, the pH, and the distribution of Cu^{2+}, $Cu(OH)^+$, $Cu(OH)_2$, $Cu(OH)_3^-$, and $Cu(OH)_4^{2-}$.

The ionic reactions and zeta potential changes in aqueous solutions are used to investigate the changes in zeta potential with time, as shown in Fig. 3. The results in Fig. 3 show that the zeta potential values fluctuate with respect to time as a result of the complex reactions in solution. However, an overall trend in the zeta potential can be observed. From 0 to 5 min, the potential shows an upward trend, increasing from −1.13 to −0.5 mV. The initial pH is 5.37.

During the experiment, the pH continues to rise and the solution became more alkaline. This indicates that the concentrations of metal ions in the aqueous solution decrease. We attribute the decrease in metal ion concentration to ion adsorption on the mineral surface, which affects the zeta potential. From 7 to 20 min, the potential increases more slowly, and achieves equilibrium at 18 min; the potential is approximately −0.3 mV. From 7 to 20 min, the pH is essentially unchanged, at approximately 7.7, indicating that various reactions in solution achieve equilibrium. The zeta potential gradually increases until stability is attained. The changes in the zeta potential indicate that hydrogen

ions or metal ions in the solution are continuously adsorbed on the mineral surface.

Previous studies suggested that the effects of copper ions on sulfide ore flotation are related to pH. In an acidic medium, a replacement reaction occurs between copper ions and sulfide minerals. In contrast, under neutral and alkaline conditions, copper ions in the form of copper hydroxides are rapidly adsorbed or precipitated on surfaces to generate CuS [37]. In this work, the water used is pure and neutral, and therefore if copper hydroxyl complexes or copper hydroxides are generated and adsorbed on the surfaces, the equilibrium pH decreases. However, in the adsorption process, the pH is neutral to mildly alkaline, and the experimental results do not agree with those from previous studies. Although hydroxyl compounds of copper are observed under alkaline conditions, the copper ion activation of sphalerite, pyrite, and other sulfide minerals mainly produce Cu–S products, which do not affect the pH [38–40].

The changes in the zeta potential in these experiments suggest that adsorption may occur between metal ions and mineral surfaces. It is reported in the literature that chalcopyrite is dissolved during crushing and grinding, resulting in a sulfur-rich surface by relaxation and reconstruction. The surface reaction primarily depends on sulfur, and then on metal atoms. Many surface reactions lead to the release of sulfur from chalcopyrite [41].

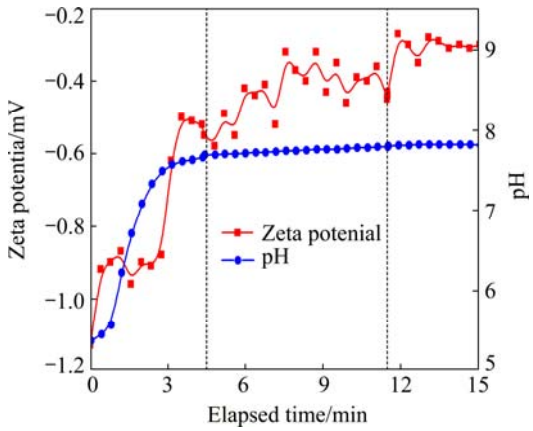

Fig. 3 Changes in zeta potential of untreated chalcopyrite solution with time

To verify the impact of copper ions on the zeta potential, the zeta potential of an aqueous solution of a fresh sample was allowed to achieve stability. Copper ions were then artificially added to the solution, using a $CuSO_4·5H_2O$ solution with a Cu^{2+} concentration of 1.4×10^{-4} mol/L. The results are shown in Fig. 4.

Figure 4 shows that after the addition of copper ions, the zeta potential increases compared with that in Fig. 3. The average potential is −0.2 mV, and the potential shows a positive trend and the solution pH decreases to 6.65. Compared with those in Fig. 3, the results in Fig. 4 show that copper ions undergo hydrolysis in aqueous solution. The solution shows weak acidity, indicating that the amount of copper ions adsorbed on the surface reaches saturation. As shown in Fig. 5, further addition of copper ions does not change the equilibrium potential, but the pH decreases gradually.

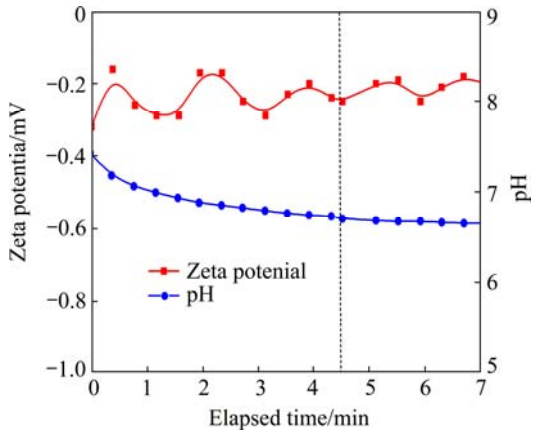

Fig. 4 Changes in zeta potential with time in addition of copper ions

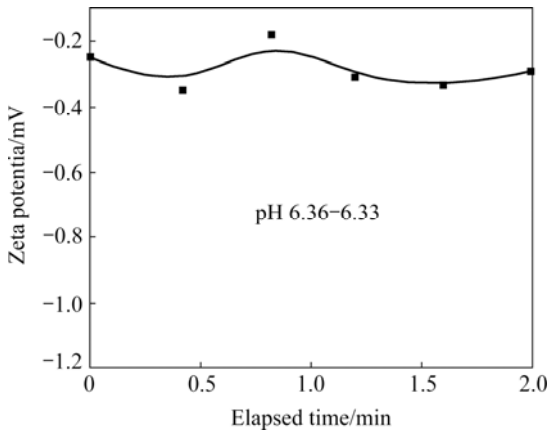

Fig. 5 Changes in zeta potential with time in addition of excess copper ions

Zeta potential trends reflect the stabilizing tendency of ion adsorption. A comparison of the adsorption and hydrolysis processes suggests that a large amount of unavoidable ions are present in the solution, particularly copper ions. The effects of these ions on the zeta potential are mainly caused by adsorption.

3.2 Copper ion adsorption experiments

The results of copper ion adsorption experiments are shown in Fig. 6. The results show that the copper ion concentration (c_{Cu}) in the solution declines from 100×10^{-6} mol/L to 46.0×10^{-6} mol/L within 0.5 min, to 2.6×10^{-6} mol/L at 3 min, and declines further to 1.2×10^{-6} mol/L

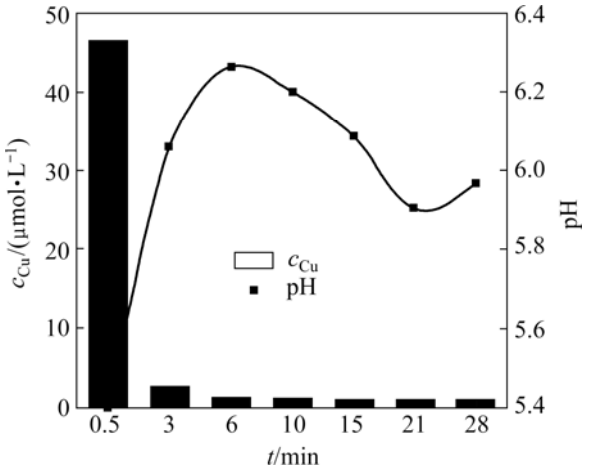

Fig. 6 Experimental results for copper ion adsorption

at 6 min. c_{Cu} decreases steeply within the first 3 min. After 15 min, c_{Cu} remaines almost unchanged, and the reactions in solution achieve equilibrium. This time is consistent with that for equilibrium of the zeta potential.

The copper ions in solution mainly exist as Cu^{2+} and a small amount of $Cu(OH)^+$ and $Cu(OH)_2$, with $Cu(OH)^+$ and $Cu(OH)_2$ appearing at pH>5.5 and pH>6.5, respectively. At pH≤5.5, the copper in solution exists as dissociated Cu^{2+}. At pH 7.32−10.68, the hydrolysis of copper ions is the highest, namely 0.066 mg/L, i.e., 1.00×10^{-6} mol/L [36]; at pH less than 7.32 or greater than 10.68, the hydrolysis of copper ions decreases [36]. The decrease in the amount of copper ions in this experiment is therefore inferred to be mainly attributable to adsorption of copper ions on the chalcopyrite surface.

3.3 XPS analysis

Figure 7 shows XP spectra of the untreated and treated chalcopyrite. Figures 7(a) and (b) show the full spectra of chalcopyrite before and after treatment, Figures 7 (c) and (e) show S 2p and Cu 2p spectra of the untreated chalcopyrite, and Figures 7 (d) and (f) show S 2p and Cu 2p spectra of the chalcopyrite treated with copper ions. The results confirm that the copper concentration on the surface increases, but the sulfur concentration decreases. The same results are obtained from the relative intensities of Cu 2p and S 2p in the full spectrum. Semiquantitative analyses of the relative atomic concentrations on the surface indicate that the copper concentration increases from 32.56% to 39.42%, and the sulfur concentration decreases from 49.11% to 41.02%. These results show that copper ions are adsorbed on the surface, leading to an increase in the copper concentration on the surface.

Figure 7 shows that the position of the S 2p peak changes, indicating a change in the binding energy to that of S^{2-}, showing that Cu–S species exist on the surface [7,42].

3.4 First-principles calculations

The adsorption energy is calculated according to the following equation:

$$E_{ads-Cu(II)/CuFeS_2(001)} = E_{Cu(II)/CuFeS_2(001)} - E_{CuFeS_2(001)} - E_{Cu(II)} \quad (16)$$

where $E_{Cu(II)/CuFeS_2(001)}$ is the total energy of the adsorption system; $E_{CuFeS_2(001)}$ is the total energy of the chalcopyrite; $E_{Cu(II)}$ is the total energy of copper chloride.

The most stable adsorption structure is shown in Fig. 8(a). Regardless of the initial position of the adsorbate, the copper atom interacts with the sulfur atom on the surface. The Cu—S (surface) bond length is 2.230 Å. The adsorption energy is −23.986 kJ/mol. The Mulliken charge population shows that the Mulliken charges of the copper atom in $CuCl_2$ before and after adsorption are 0.26e and 0.40e, respectively. These results indicate electron exchange between copper and surface sulfur. During adsorption, electrons are transferred to $CuCl_2$ via surface sulfur.

Figure 8(b) shows the charge density difference plot for the adsorption system. The light color represents the region with low electron density and the dark color represents the region with high electron density. Figure 8(b) shows the electron distributions around copper and sulfur. Based on a combination of the adsorption energy and electron distribution, we conclude that the chemical adsorption of a copper atom occurs at the sulfur atom on the surface and generates Cu—S bonds. This finding is consistent with the XPS results.

3.5 Hallimond tube flotation experiments

The experimental results for Hallimond tube flotation are shown in Fig. 9. The experimental samples were cleaned to remove the surface oxidation layer and other impurities. The influence of the copper ions on flotation was then studied. Figure 9 shows that within 20 min, the recovery rate of nonactivated chalcopyrite is 48.3%. The recovery rate of chalcopyrite activated by copper ions for 5 min increases to 57.6%. After activation for 20 min, the recovery increases to 66.1%. The recovery rate after activation for 20 min is higher than that after 5 min. However, the final recovery rates under the three conditions are similar, indicating that copper ion adsorption affects the flotation rate of chalcopyrite. These results also show that copper ions interact with the surface, and adsorption is beneficial to flotation. The results of the Hallimond tube flotation experiments show that copper ions are adsorbed on the surface. This adsorption promotes interactions between

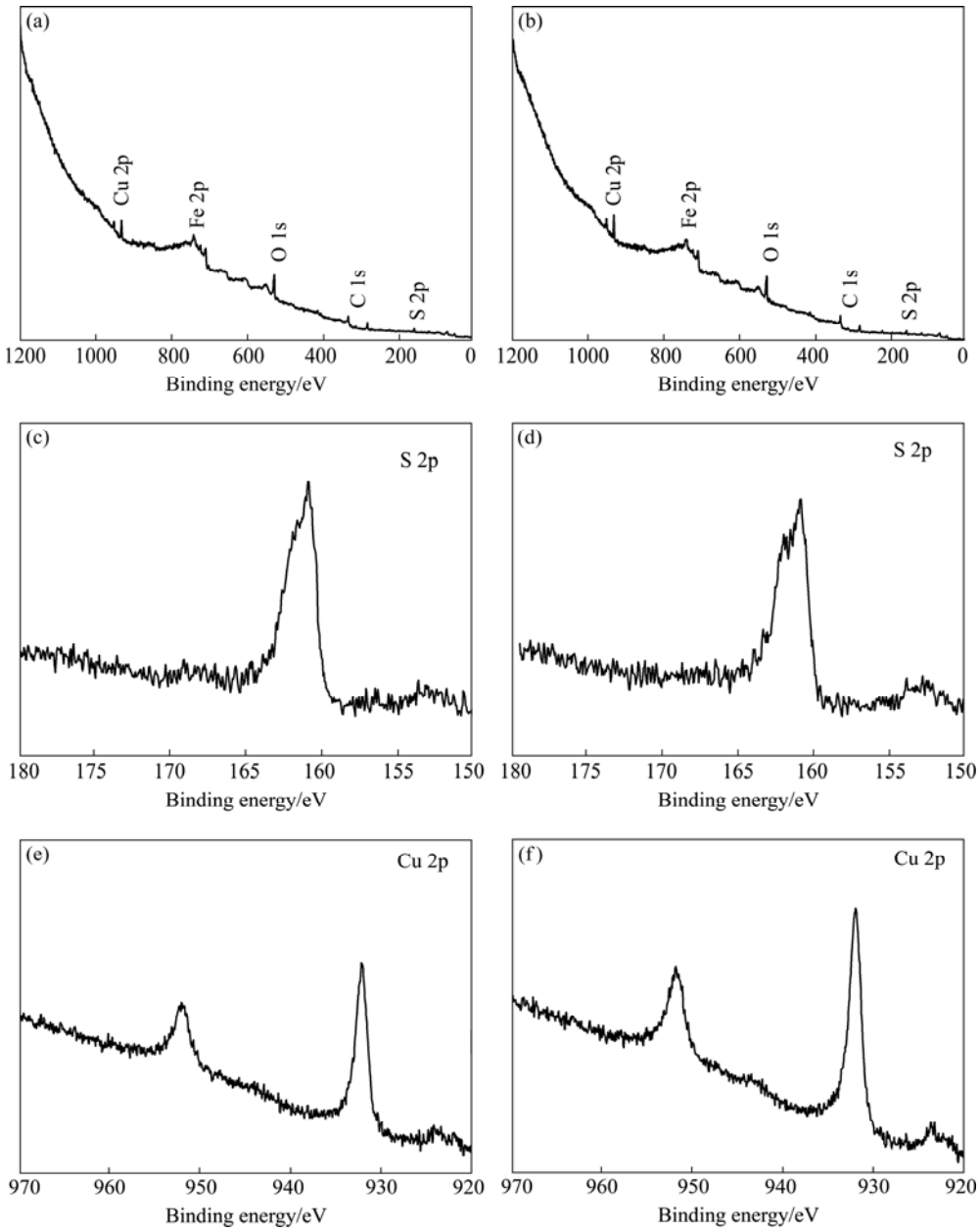

Fig. 7 XP spectra of untreated and treated chalcopyrite: (a) Full spectrum, untreated; (b) Full spectrum, treated; (c) S 2p spectrum, untreated; (d) S 2p spectrum, treated; (e) Cu 2p spectrum, untreated; (f) Cu 2p spectrum, treated

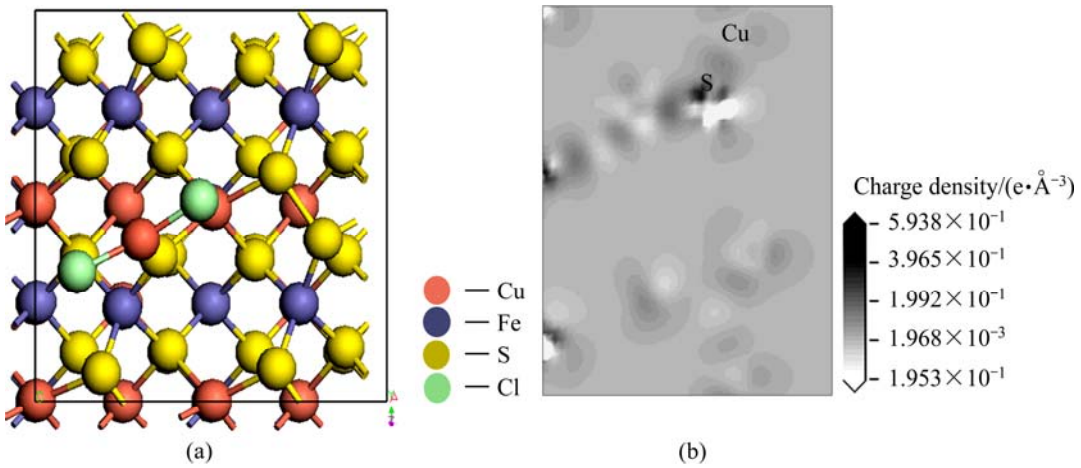

Fig. 8 Stable adsorption structure (a) and charge density difference plot of adsorption system (b)

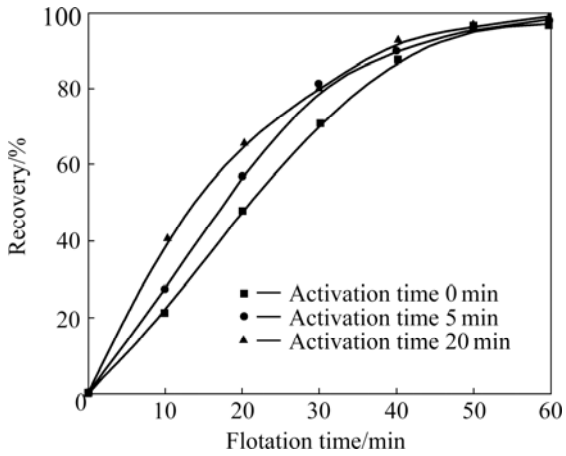

Fig. 9 Hallimond tube flotation experiments on chalcopyrite

the surface and ethyl xanthate, i.e., the copper ions activate the chalcopyrite. The experiments are conducted using an adequate ethyl xanthate concentration, otherwise xanthate copper formation would adversely affect the recovery rate.

4 Conclusions

1) The XPS results show that the ratio of copper to sulfur atoms on the chalcopyrite surface increases. Combined with the changes in the zeta potential, the displacement of the binding energy of the sulfur atom shows that chemical adsorption of the copper ions at sulfur atoms on the surface occurs.

2) First-principles calculations show that the adsorbed copper reacts with the surface sulfur, further affecting the electronic structures of the second and inner layers. The adsorption energy is −23.986 kJ/mol. The Mulliken charge population and charge density difference plot show that more electrons are distributed around copper and sulfur. Electron exchange occurs between copper and surface sulfur. Chemical adsorption of copper on surface sulfur atoms generates Cu—S bonds.

3) Under certain conditions, the adsorption of copper ions on the surface is conducive to chalcopyrite flotation.

References

[1] ZHANG Q, XU Z, BOZKURT V, FINCH J A. Pyrite flotation in the presence of metal ions and sphalerite [J]. Int J Miner Process, 1997, 52(2−3): 187−201.

[2] FINKELSTEIN N P. The activation of sulphide minerals for flotation: A review [J]. Int J Miner Process, 1997, 52(2−3): 81−120.

[3] CHANDRA A P, GERSON A R. A review of the fundamental studies of the copper activation mechanisms for selective flotation of the sulfide minerals, sphalerite and pyrite [J]. Adv Colloid Interfac, 2009, 145(1−2): 97−110.

[4] GERSON A R, LANGE A G, PRINCE K E, SMART R S C. The mechanism of copper activation of sphalerite [J]. Appl Surf Sci, 1999, 137(1−4): 207−223.

[5] CHEN Z, YOON R H. Electrochemistry of copper activation of sphalerite at pH 9.2 [J]. Int J Miner Process, 2000, 58(1−4): 57−66.

[6] FOMASIERO D, RALSTON J. Cu(II) and Ni(II) activation in the flotation of quartz, lizardite and chlorite [J]. Int J Miner Process, 2005, 76(1−2): 75−81.

[7] POPOV S R, VUCINIC D R. The ethylxanthate adsorption on copper-activated sphalerite under flotation-related conditions in alkaline media [J]. Int J Miner Process, 1990, 30(3−4): 229−244.

[8] PATTRICK R A D, ENGLAND K E R, CHARNOCK J M, MOSSELMANS J F W. Copper activation of sphalerite and its reaction with xanthate in relation to flotation: An X-ray absorption spectroscopy (reflection extended X-ray absorption fine structure) investigation [J]. Int J Miner Process, 1999, 55(4): 247−265.

[9] BOULTON A, FORNASIERO D, RALSTON J. Characterisation of sphalerite and pyrite flotation samples by XPS and ToF-SIMS [J]. Int J Miner Process, 2003, 70(1−4): 205−219.

[10] WEISENER C, GERSON A. Cu(II) adsorption mechanism on pyrite: An XAFS and XPS study [J]. Surf Interface Anal, 2000, 30(1): 454−458.

[11] WANG Zhao-hui, XIE Xue-hui, LIU Jian-she. Experimental measurements of short-term adsorption of *Acidithiobacillus* ferrooxidans onto chalcopyrite [J]. Transactions of Nonferrous Metals Society of China, 2012, 22(2): 442−446.

[12] LIN Hui-bo, YIN Wan-zhun, SUN Chuan-yao. XPS analysis on adsorption law of metal ion on surface of silicate minerals [J]. Non-ferrous Mining and Metallurgy, 2003, 19(3): 21−24. (in Chinese)

[13] ZENG Qing-hua, ZHAO Hong, WANG Dian-zuo. Influence of metal cations on cassiterite flotation [J]. Transactions of Nonferrous Metals Society of China, 2000, 10(1): 98−101.

[14] DENG Jiu-shuai, WEN Shu-ming, XIAN Yong-jun, LIU Jian, LIU Dan. Spectroscopic characterization of dissolubility and surface properties of chalcopyrite in aqueous solution [J]. Spectrosc Spectral Anal, 2012, 32(2): 519−524. (in Chinese)

[15] HIDALGO J L, GOMEZ M A, CABALLERO M, CELA R, PEREZ-BUSTAMANTE J A. Determination of Mo(VI) in tap-water and sea-water by differential-pulse polarography and co-flotation [J]. Talanta, 1988, 35(4): 301−305.

[16] CORIN K C, REDDY A, MIYEN L, WIESE J, HARRIS P. The effect of ionic strength of plant water on valuable mineral and gangue recovery in a platinum bearing ore from the Merensky reef [J]. Miner Eng, 2011, 24(2): 131−137.

[17] CABEZON L M, CABALLERO M, CELA R, PEREZ-BUSTAMANET J A. Simultaneous separation of copper, cadmium and cobalt from sea-water by co-flotation with octadecylamine and ferric hydroxide as collectors [J]. Talanta, 1984, 31(8): 597−602.

[18] COETZER G, du PREEZ H S, BREDENHANN R. Influence of water resources and metal ions on galena flotation of Rosh Pinah ore [J]. J S Afr Inst Min Metall, 2003, 103(3): 193−201.

[19] CHEN Jian-ming, LIU Run-qing, SUN Wei, QIU Guan-zhou. Effect of mineral processing wastewater on flotation of sulfide minerals [J]. Transactions of Nonferrous Metals Society of China, 2009, 19(2): 454−457.

[20] DENG Jiu-shuai, WEN Shu-ming, XIAN Yong-jun, LIU Jian, BAI Shao-jun. New discovery of unavoidable ions source in chalcopyrite flotation pulp: Fluid inclusions [J]. Miner Eng, 2012, 42: 22−28.

[21] KELEBEK S, SMITH G W. Electrokinetic properties of a galena and chalcopyrite with the collectorless flotation behaviour [J]. Colloids Surf, 1989, 40(1−2): 137−143.

[22] PENG Y, ZHAO S. The effect of surface oxidation of copper sulfide minerals on clay slime coating in flotation [J]. Miner Eng, 2011,

24(15): 1687−1693.
[23] KRESSE G, FURTHMULLER J. Software VASP, Vienna (1999) [J]. Phys Rev B, 1996, 54: 169−171.
[24] KRESSE G, FURTHMULLER J. Vienna Ab-initio simulation package [M]. Vienna: University of Wien, 2001: 1.
[25] KRESSE G, JOUBERT D. From ultrasoft pseudopotentials to the projector augmented-wave method [J]. Phys Rev B, 1999, 59(3): 1758−1775.
[26] PERDEW J P, CHEVARY J A, VOSKO S H, JACKSON K A, PEDERSON M R, SINGH D J, FIOLHAIS C. Atoms, molecules, solids, and surfaces: Applications of the generalized gradient approximation for exchange and correlation [J]. Phys Rev B, 1992, 46(11): 6671−6679.
[27] PERDEW J P, YUE W. Accurate and simple density functional for the electronic exchange energy: Generalized gradient approximation [J]. Phys Rev B, 1986, 33: 8800−8802.
[28] BLOCHL P E. Projector augmented-wave method [J]. Phys Rev B, 1994, 50: 17953−17979.
[29] MONKHORST H J, PACK J D. Special points for Brillouin-zone integrations [J]. Phys Rev B, 1976, 13: 5188−5192.
[30] BLOCHL P E, JEPSEN O, ANDERSEN O K. Improved tetrahedron method for Brillouin-zone integrations [J]. Phys Rev B, 1994, 49(23): 16223−16233.
[31] FEYNMAN R P. Forces in molecules [J]. Phys Rev, 1939, 56: 340−342.
[32] TCHISTIAKOV A A. Colloid chemistry of in-situ clay-induced formation damage [C]// Proceedings of SPE International Symposium On Formation Damage Control. Louisiana: Society of Petroleum Engineers Lafayette, 2000: 371−379.
[33] JONES M H, WOODCOCK J T. Principles of mineral flotation [C]// Parkville, Australasian Inst of Mining & Metallurgy, 1984: 43−45.
[34] HEYES G W, TRAHAR W J. The natural flotability of chalcopyrite [J]. Int J Miner Process, 1977, 4(4): 317−344.
[35] WANG Dian-zuo, HU Yue-hua. Solution chemistry of flotation [M]. Changsha: Hunan Science & Technology Press, 1988: 10−30. (in Chinese)
[36] CHANG Hao, CHAI Li-yuan, WANG Yun-yan, SHU Yu-de, ZHOU Min. Study on equilibrium of hydroxyl complex ions in Cu^{2+}–H_2O system [J]. Min Metall Eng, 2007, 27(6): 37−40. (in Chinese)
[37] TANG Lin-sheng, HUANG Kai-guo, WANG Dian-zuo. Effect machanism of cooper ions on sulphie ores–a study [J]. Min Metall Eng 1989, 3(3): 29−32.
[38] BUCKLEY A N, WOODS R, WOUTERLOOD H J. The deposition of sulfur on pyrite and chalcopyrite from sodium sulfide solutions [J]. Aust J Chem, 1988, 41(7): 1003−1111.
[39] VOIGT S, SZARGAN R, SUONINEN E. Interaction of copper (II) ions with pyrite and its influence on ethyl xanthate adsorption [J]. Surf Interface Anal, 1994, 21(8): 526−536.
[40] LAAJALEHTO K, LEPPINEN J, KARTIO I, LAIHO T. XPS and FTIR study of the influence of electrode potential on activation of pyrite by copper or lead [J]. Colloids Surf, A, 1999, 154(1−2): 193−199.
[41] HAYES R A, PRICE D M, RALSTON J, SMITH R W. Collectorless flotation of sulphide minerals [J]. Miner Process Extr Metall Rev, 1987, 2(3): 203−208.
[42] FORNASIERO D, RALSTON J. Effect of surface oxide/hydroxide products on the collectorless flotation of copper-activated sphalerite [J]. Int J Miner Process, 2006, 78(4): 231−237.

铜离子在黄铜矿表面的吸附及活化作用：一个自活化的新观点

邓久帅，文书明，刘 建，吴丹丹，丰奇成

昆明理工大学 国土资源工程学院，复杂有色金属资源清洁利用国家重点实验室，昆明 650093

摘 要：通过 Zeta 电位分析、X 射线光电子能谱分析、铜离子吸附试验、第一性原理计算及 Hallimond 浮选试验综合揭示了铜离子在黄铜矿表面同样存在着吸附行为，铜离子对黄铜矿同样具有活化作用，主要诱因是铜离子与表面活化位的硫作用，从而增加疏水性。这种吸附作用在一定条件下有利于黄铜矿自身的浮选。浮选矿浆中的铜离子主要来源于黄铜矿的表面氧化溶解和矿物内流体包裹体的释放，这些离子的存在及吸附使黄铜矿具有自活化特性。

关键词：黄铜矿；铜离子；吸附；自活化

(Edited by Yun-bin HE)